JPE 9-1-3

A Fuel Cell Generation System with a New Active Clamp Sepic-Flyback Converter

Won-Cheol Lee*, Su-Jin Jang**, Soo-Seok Kim***, Su-Won Lee* and Chung-Yuen Won†

†*School of Information and Communication Engineering, Sungkyunkwan University, Suwon, Korea
**Hyosung Industry Research Center, Anyang, Korea
***Department of Electrical Engineering, Seoul National University of Technology, Seoul, Korea

ABSTRACT

A high efficiency active clamp sepic-flyback converter is presented for fuel cell generation systems. The proposed converter is a superposition of a sepic converter mode and flyback converter mode. The output voltages of the sepic converter mode and flyback converter mode can be regulated by the same PWM technique with constant frequency. By merging the sepic and flyback topologies, they can share the transformer, power MOSFET and active clamp circuit. The result has outstanding advantages over conventional active clamp DC-DC converters: high efficiency, high power density, and component utilization. Simulation results and experimental results are presented to verify the principles of operation for the proposed converter.

Keywords: Active clamp, Sepic-flyback converter, Fuel cell generation system

1. Introduction

The fuel cell is an electrochemical device that converts chemical energy directly into electrical and thermal energies. Fuel cells are starting to meet the power needs of a variety of applications. Furthermore, the fuel cell is regarded as a good alternative renewable energy source that solves serious problems with other energy sources such as the exhausting of fossil energy and severe environmental pollution of some energy sources.

Manuscript received June 30, 2008; revised October 15, 2008
†Corresponding Author: won@yurim.skku.ac.kr
Tel: +82-31-290-7115, Fax: +81-31-299-4623, Sungkyunkwan Univ.
*School of Information and Communication Eng., Sungkyunkwan Univ.
**Hyosung Industry Research Center
***Dept. of Electrical Eng., Seoul National Univ. of Tech

The basic feature of a fuel cell stack is that it is composed of individual low voltage cells. A minimum number of cells make the best sense from a cost standpoint.

Furthermore, manufacturers of fuel cell generation systems have been using a low voltage, 28~43[Vdc], as a standard output voltage. This low voltage characteristic requires that the output voltage of the fuel cell stack is boosted before it is inverted to an AC source. Therefore, the inverter must have a DC-DC converter on the front-end[1,2].

The flyback topology has been attractive for a long time because of its relative simplicity when compared with other topologies used in low power (up to several hundred watts) applications. The transformer of a flyback converter serves the dual purposes of providing energy storage as

well as acting as a converter.

The demerits of the flyback converter are its relatively high voltage and current stress generated in its switching components. High peak RMS current stress is a particular problem during operation in a discontinuous conduction mode (DCM). This problem causes a primary loss to increasing output power[3,4,5].

For this reason, this paper applies sepic-flyback converter topology into a fuel cell generation system. In the sepic-flyback converter, a transformer core is used well as a push-pull, full-bridge, and half-bridge converters. Furthermore this topology has high efficiency, high power density, and other advantages. When the main switch is on, the input energy is transferred to the output circuit by the sepic mode and when the main switch is off, the leakage inductance energy is transferred to the output circuit by the flyback mode.

In other words, the sepic-flyback converter can be transferred to energy twice as much as other conventional topologies during one switching period. Also, the active clamp circuits are used to clamp the voltage spikes of the switch and to recycle the energy in the leakage inductance of the power transformer[6,7].

The zero voltage switching (ZVS) zeta-flyback converter, connected in parallel to the load, has been studied to increase the output power by combining the output currents of the two topologies[8].

In this paper, the output circuit in the sepic and flyback topologies was connected in series to the load to obtain high output voltage by separating the turn ratio of the secondary side windings. The proposed converter boosts the low output voltage (28~43[Vdc]) of the fuel cell stacks to a high DC voltage such as 380[Vdc]. The developed converter is tested with a 1.2[kW] Ballard Nexa Proton Exchange Membrane (PEM) fuel cell stack, so that the validity of the proposed generation system is verified experimentally.

2. Proposed Fuel Cell Generation System

The configuration of the fuel cell generation system with the proposed active clamp sepic-flyback converter is depicted in Fig. 1. The developed fuel cell system consists of a PEM fuel cell (Ballard Nexa), an active clamp DC-DC sepic-flyback converter, and a conventional full bridge DC-AC inverter. The controller of the full bridge DC-AC inverter consists of a DSP(TMS320C31,TI) which processes the voltage feedback signal and an I/O control unit. Utilization of a sinusoidal PWM control technique allows for constant voltage and constant frequency in the output voltage of the inverter.

2.1 The active clamp sepic-flyback converter

Fig. 1 shows a new fuel cell generation system with a new active clamp sepic-flyback converter. In order to reduce the winding ratio of the transformer, switching stresses on the main switch and auxiliary switch or active clamp switch, the primary sides of the proposed sepic-flyback converters were connected to each other in a parallel manner. On the other hand, the secondary side of the converter was in a series connection.

In this paper, we propose an improved fuel cell

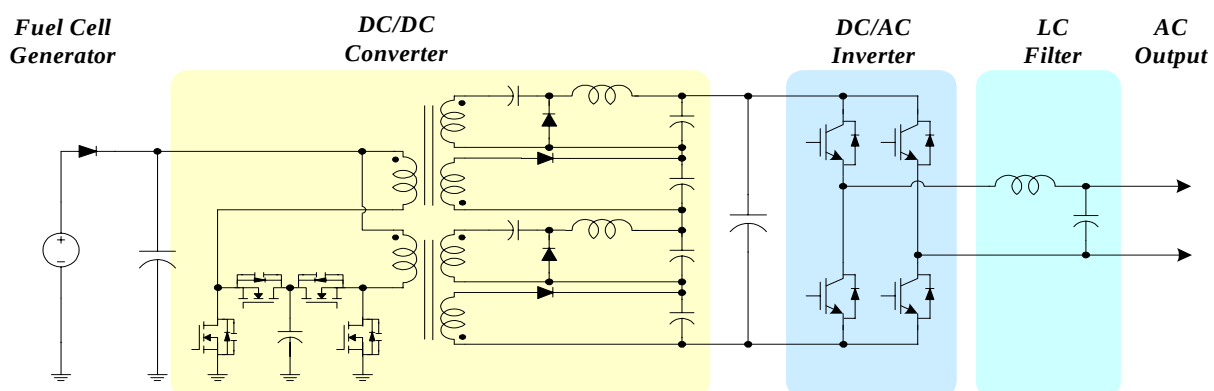

Fig. 1 The configuration of a fuel cell generation system

generation system by compensating for problems of conventional sepic-flyback converters.

Fig.2 (a) shows the conventional sepic-flyback converter. In this topology, a sepic converter and a flyback converter are merged by utilizing a center-tap transformer. As a result, the transformer utilization ratio and energy transfer density of this topology are high by reducing the turn ratio of the transformer. When the conventional sepic-flyback converter is operating in flyback mode, it has the possibility of demagnetizing in the sepic winding by the stored energy at C_1. In fact, this problem is caused by the common center-tap of the transformer.

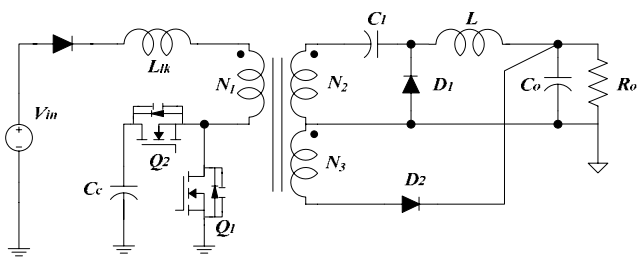

(a) Conventional sepic-flyback converter

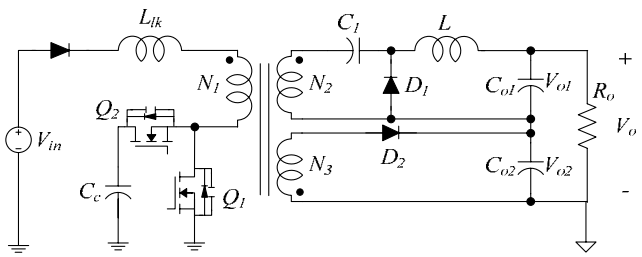

(b) proposed sepic-flyback converter

Fig. 2 The active clamp sepic-flyback converter

As shown in Fig. 2(b), the proposed converter divides the center-tap to reduce interferences on the common center-tap. So the loss caused by the interference is reduced [8].

Therefore, the proposed active clamp sepic-flyback converter was designed to separate the center tap to minimize the interference generated by using a common center tap transformer.

The active clamp sepic-flyback converter performs DC/DC conversion that is similar to the operation of the buck-boost converter whose output DC voltage can be regulated by the duty ratio.

2.2 The behavior of the active clamp sepic-flyback converter

Fig.3 shows the waveforms of the steady state operation of the proposed converter topology. Also this figure shows the time sequence of gate drive voltages for switches, Q_1 and Q_2, the main switch voltage V_{DS}, the main switch current I_{S1}, the auxiliary switch current I_{S2}, the current through D_1 and D_2, and the inductor current I_L.

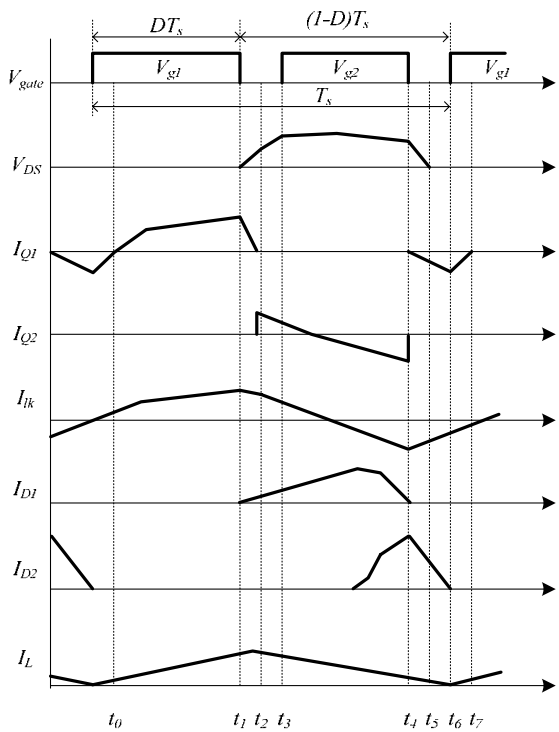

Fig. 3 Steady state waveforms of the proposed converter

Fig. 4 illustrates the operation stages for the active clamp sepic-flyback converter. The proposed converter can operate in the different 4 stages characterized by different time sequences from t_0 to t_7 in a switching period. For a brief description of circuit operation, we make the following assumptions:

1) An ideal switch with body diode
2) A steady-state continuous current mode (CCM)

Stage 1: Main switch conduction

(t_0 - t_1) : At the beginning of this stage, the main switch Q_1 is turned on at t_0. The clamp capacitor (charged to V_{Cc})

is disconnected from the equivalent circuit, as shown in Fig. 4(a). The input voltage V_{in} is applied to the primary winding of the transformer. The input energy is connected to the capacitor C_1 through a transformer and the energy is stored in the inductor L. The diode D_2 is reverse-biased at this stage.

Stage 2: Turn off transition

(t_1 - t_2) : When the main switch Q_1 is turned off, the parasitic capacitor of the main switch C_{Q1} charges up to the forward bias point of the body diode of the auxiliary switch D_{Q2}, as shown in Fig. 4(b).

(t_2 - t_3) : At t_2, the voltage across the main switch V_{DS} is $V_{in} + V_o \times (N_2/N_1)$. When the body diode of the auxiliary switch D_{Q2} is turned on, the current through the body diode stores energy in Cc, as shown in Fig. 4(c).

Stage 3: Clamp circuit operation

(t_3 - t_4) : During this stage, the clamp circuit (Q_2, Cc) provides a low impedance path for the leakage inductance energy. When the active clamp switch's body diode D_{Q2} conducts, the active clamp capacitor Cc is charged while negative voltage appears across the primary side of the transformer, as shown in Fig. 4(d).

At the same time, the flyback mode diode D_2 is turned on. Its current increases slowly due to the presence of the leakage inductance. The freewheeling diode of the sepic mode is turned on. The clamp circuit current decreases in a resonant manner. Once the clamp circuit current reaches zero, it is allowed to reverse if the active clamp switch Q_2 has been turned on. For the duration of the active clamp switch Q_2 conduction, the stored energy of the active clamp capacitor Cc is transferred back to the magnetizing and leakage inductance. The active clamp capacitor is discharged back to its steady state value. Most of the magnetizing energy is being transferred to the output during this stage.

Stage 4: Turn on transition

(t_4 - t_5) : The equivalent circuits for stage 4 are shown in Fig. 4(e)~(f).When the active clamp switch Q_2 is turned off, the reverse current, flowing in the leakage and magnetizing inductances, starts to discharge to C_1.

(t_5 - t_7) : When the parasitic capacitor C_{Q1} of the main switch is completely discharged the body diode is turned on. To achieve a zero voltage turn on the main switch Q_1 is turned on. At the end of this stage, one switching cycle is completed.

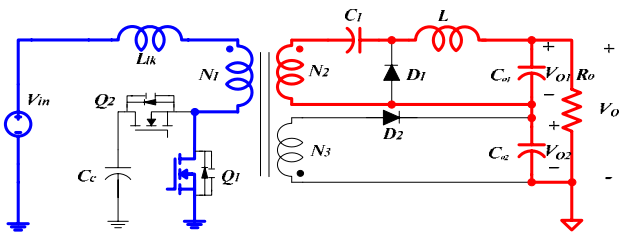

(a) $t_0 \sim t_1$

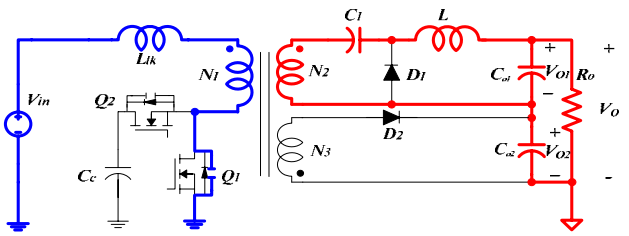

(b) $t_1 \sim t_2$

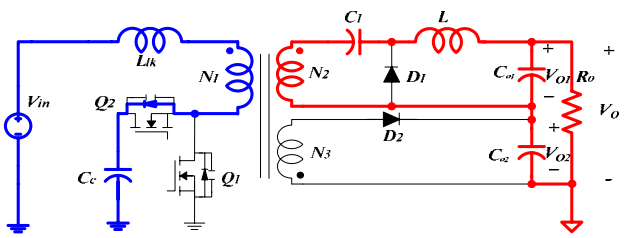

(c) $t_2 \sim t_3$

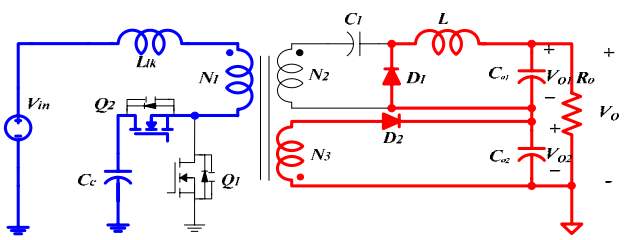

(d) $t_3 \sim t_4$

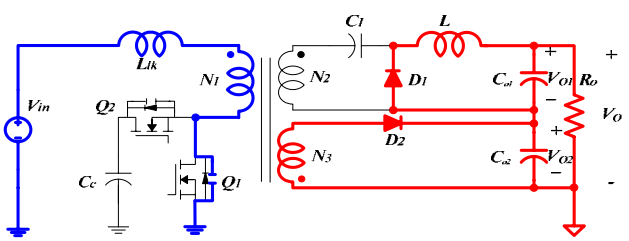

(e) $t_4 \sim t_5$,

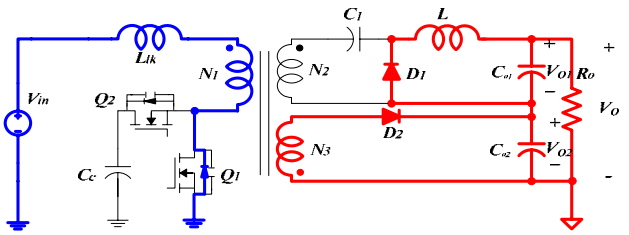

(f) $t_5 \sim t_7$

Fig. 4 Operation stages of the active clamp sepic-flyback converter

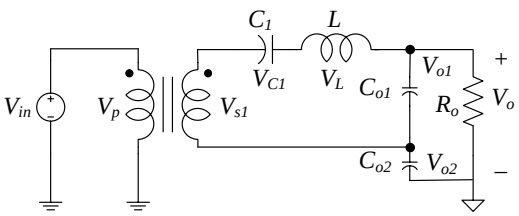

(a) ($t_0 \sim t_1$)

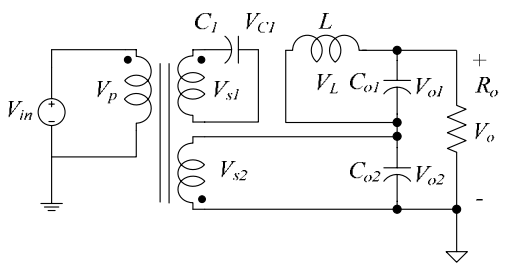

(b) ($t_3 \sim t_4$)

Fig. 5 The equivalent circuit of the active clamp sepic-flyback converter

2.3 Design consideration

Fig. 5 (a) shows equivalent circuits at the conduction stage of the main switch.

We have obtained Eq. (1) by using Kirchhoff's Voltage Law(KVL).

$$V_{o1} + V_{o2} = V_o \tag{1}$$

Fig. 5(b) shows an equivalent circuit at the turn off of Q_1. Applying the same assumption, the expression of V_{in} and V_p is as follows:

$$V_{in} = V_p \tag{2}$$

The induced voltage for the sepic converter V_p is given by

$$V_p = \frac{N_p}{N_{s1}} V_{s1} \tag{3}$$

By KVL in the sepic converter of Fig. 5(b), the expression of V_{s1} and V_{c1} are as follows:

$$V_{s1} + V_{c1} = 0 \tag{4}$$

By KVL in the flyback converter of Fig. 5(b), we obtain the following equation.

$$V_{s2} - V_{o2} = 0 \tag{5}$$

The induced voltage at the flyback winding is given by

$$V_p = -\frac{N_p}{N_{s2}} V_{s2} \tag{6}$$

To find the steady state condition in the proposed converter, the average inductor voltage V_L is zero in steady state.

According to the duty ratio, the secondary side voltage of the flyback converter can be found as follows:

$$V_{s2} = \frac{N_{s2}}{N_p} \frac{D}{1-D} V_{in} \tag{7}$$

$$V_{s2} = V_{o2} \tag{8}$$

where D is the duty ratio. Therefore, the output voltage in the flyback converter mode can be derived as Eq. (9). In this equation, the output voltage is equivalently the same as the buck-boost converter.

$$V_{o2} = \frac{N_{s2}}{N_p} \frac{D}{1-D} V_{in} \tag{9}$$

According to the duty ratio, the output voltage and the secondary side voltage of the sepic converter can be found as Eqs. (10) and (11).

The output voltage in the sepic converter mode is given as Eq. (14). It is also equivalently the same as the buck-boost converter.

$$V_{o1} = \frac{D}{1-D} V_{s1} \tag{10}$$

$$V_{s1} = \frac{N_2}{N_1} V_{in} \tag{11}$$

$$V_{o1} = \frac{N_2}{N_1} \frac{D}{1-D} V_{in} \tag{12}$$

According to steady state analysis of the sepic-flyback converter, the output voltage is concluded by using Eqs. (9) and (12). So the output voltage of the sepic-flyback converter is given by Eq. (13).

$$V_o = \frac{N_{s1} + N_{s2}}{N_p} \frac{D}{1-D} V_{in} \tag{13}$$

If N_{s1} and N_{s2} are the same in Eq. (13), V_{in} is simplified to Eq. (14). Therefore, the output voltage of the sepic-flyback converter is the same as the buck–boost converter considering the turn ratio.

$$V_{in} = 2N \frac{1-D}{D} V_o \tag{14}$$

So the conversion ratio of the proposed converter is similar to that of the buck-boost converter, but the ratio contains an added factor of N.

Where $N = \frac{N_{s1}}{N_p}$ or $N = \frac{N_{s2}}{N_p}$

According to the voltage balance condition on the transformer,

$$V_{in} DTs = (V_{Cc} - V_{in})(1-D)Ts \tag{15}$$

Solving Eq. (15), the clamp voltage V_{Cc} is

$$V_{Cc} = \frac{1}{1-D} V_{in} = \frac{V_o}{ND} \tag{16}$$

In this equation, the clamp voltage V_{Cc} is determined by the input voltage V_{in} and the duty ratio D. The maximum voltage stress of the switch is equal to the voltage across the clamp capacitor.

Therefore, the maximum voltage stress of the main switch Q_1 is given by

$$V_{DS1\max} = V_{Cc} = \frac{1}{1-D} V_{in} \tag{17}$$

The peak current stress of Q_1 is the summation of the load current and the magnetizing current.

$$I_{Q1\max} = NI_{o\max} + I_m \tag{18}$$

The block diagram of the full bridge DC-AC inverter, including the DSP (TMS320C31) control block, is described in Fig. 6. The controller of the DC-AC inverter consists of a control unit that processes the digital calculations and I/O ports.

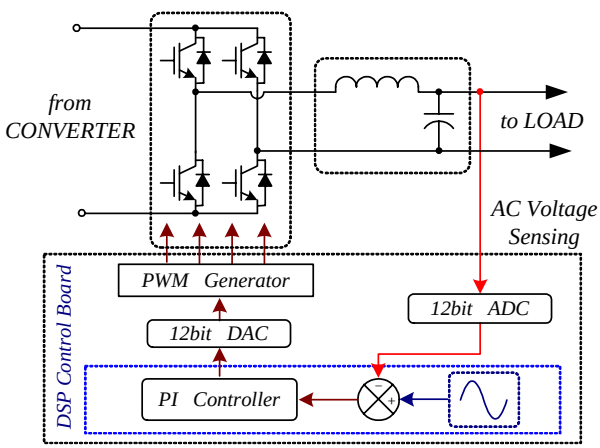

Fig. 6 A block diagram of the single phase dc-ac inverter

The inverter is controlled so as to produce a constant voltage and constant frequency. The control technique of the inverter uses the average voltage control and sinusoidal pulse with modulation(SPWM)[9,10].

3. Simulation and Experimental Results

Simulation of the proposed system has been carried out with a PSIM 6.0. Several experiments have been performed with a PEM fuel cell generator, a 1.2 [kW] module

manufactured by the Ballad Nexa. The performance of the proposed sepic-flyback converter has been verified through the simulation schematic diagram in Fig. 7.

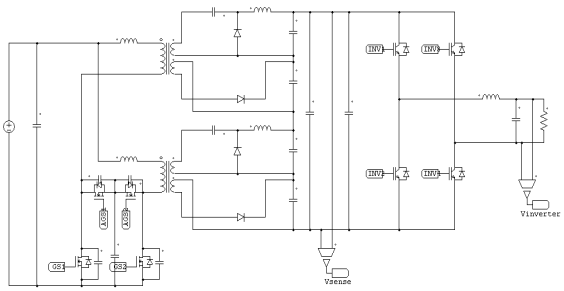

Fig. 7 A simulation schematic of the proposed fuel cell generation system

Table 1 represents the design parameters for the proposed active clamp sepic-flyback converter.

Table 1 Parameter of Sepic-Flyback Converter

Parameter	Variable	Value
Rated Power	P_o	1000[W]
Input Voltage	V_i	24-40Vdc
Output Voltage	V_o	380Vdc
Switching Frequency	f_s	100kHz
Turn Ratio of Transformer	N	1:4
Leakage inductance	Llk	6 uH
Output Inductance	L	600uH
Sepic Capacitance	$C1$	3uF
Clamping Capacitance	Cc	4uF

In the simulation and experiments, the switching frequency of the proposed converter was 100[kHz] and the single-phase inverter was operated at 4.5[kHz]. A resistor bank was connected to the output terminal of the single-phase inverter as a load.

The simulation results of the proposed DC-DC converter are shown in Fig. 8. Fig. 8 shows the behavior of the main and auxiliary switches. The main and auxiliary switches are successfully operated under the ZVS condition at the turn-on switching transients.

Fig. 8 Simulation waveforms of the proposed converter

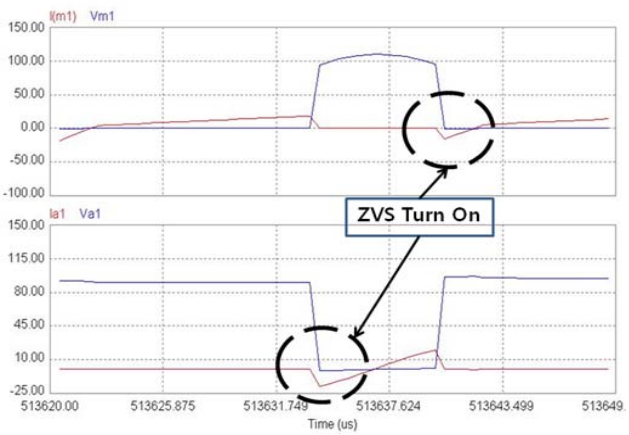

Fig. 9 Voltage and current waveforms of the main switch and the auxiliary switch.

Fig. 9 shows the ZVS condition of the main and auxiliary switches. In Fig. 8 and Fig. 9, we note that ZVS is always achieved in the main and auxiliary switches under all of the operational conditions.

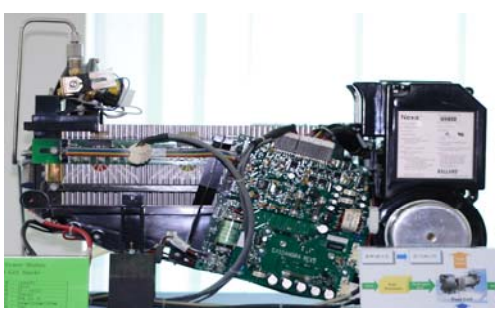

Fig. 10 The PEM fuel cell stack of the 1.2[kW] Ballard Nexa Power Module

Fig. 10 shows an output voltage and current waveforms of the inverter in case that a resistor bank is connected to the inverter output stage.

Fig. 11 shows an actual fuel cell generator (1.2[kW] Ballard Nexa Power Module) to evaluate performance through experiments.

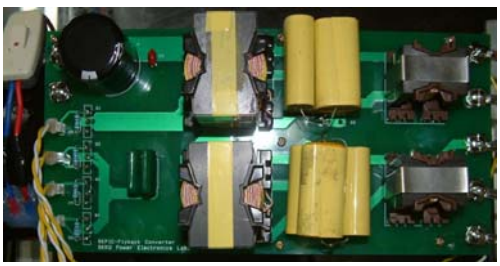

(a) Sepic-flyback converter circuit

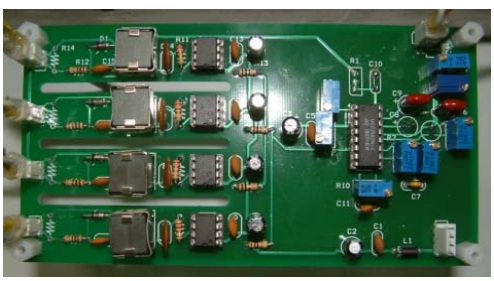

(b) Gate drive circuit

Fig. 11 The sepic-flyback converter and gate drive

Fig. 12 shows the voltage and current waveforms of *Q1* for the proposed sepic-flyback converter.

From the results, we can see that I_{Q1} flows after the V_{DS} drops to zero, meaning ZVS turn on. Due to this ZVS operation, the power loss of the converter can be reduced, so that the converter could increase the overall efficiency of the system.

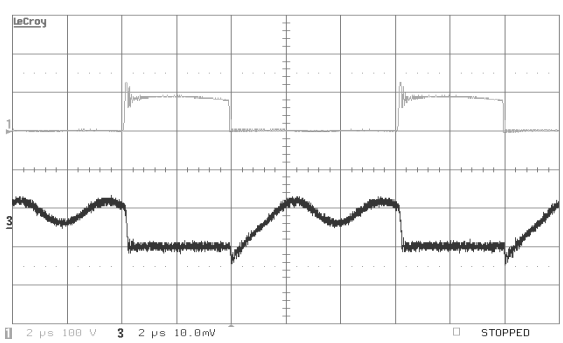

Fig. 12 The voltage and current waveforms of the main switch

With the switching signals, we note that the voltages across all of the switches are clamped to the same value of the clamp capacitor. In addition, the overshoot voltages of the switches could be eliminated successfully as shown in Fig. 12.

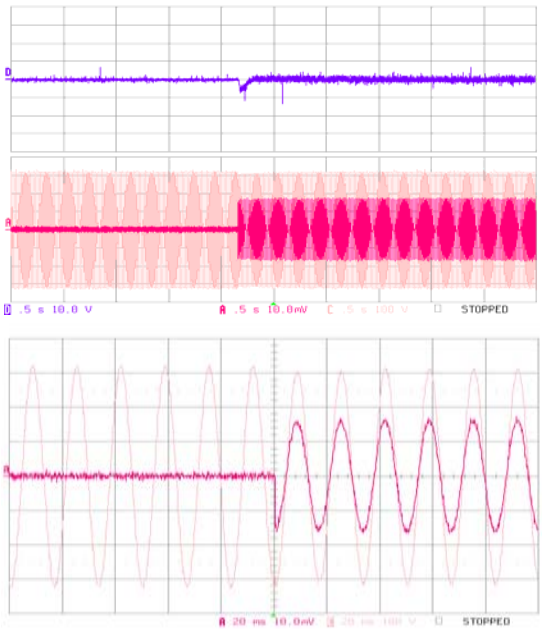

Fig. 13 The dynamic result of the proposed fuel cell generation system

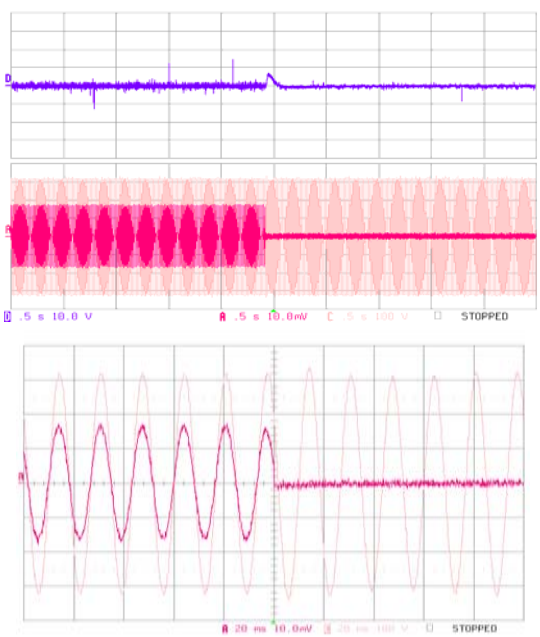

Fig. 14 The dynamic result of the proposedfuel cell generation system

The dynamic experimental results are shown in Fig. 13 and Fig. 14. They show the voltage and current output characteristics of the proposed fuel cell generation system with a real fuel cell stack when the load was changed.

For a dynamic response, the load was changed suddenly from no load to 500 [W]. Fig. 13 illustrates dynamic AC response characteristics of the DC-link and the voltage and current of inverter.

Fig. 14 shows the dynamic AC response of the proposed converter and output waveforms of the DC-AC inverter. It shows that the load was changed suddenly from 500 [W] to no load.

From the experimental results, we assert that the active clamp sepic-flyback converter generates a constant 380[V] DC output and the full-bridge DC-AC inverter successfully provides 220V/60Hz AC voltage and current into the 500 [W] resistor bank. This arrangement has low harmonics and is proper for various domestic loads.

An efficiency comparison with the proposed converter and conventional converters was performed under different load conditions as shown in Fig.15.

The proposed reduced model converter (100 [W]) has higher efficiency than conventional flyback and sepic converters. The measured efficiency is 90.18[%] at 100 [W]. Also, this converter improves the efficiency by about 3% in comparison with an active clamp sepic converter at same condition.

Fig. 16 shows the measured efficiency of the proposed 1 [kW] active clamp sepic-flyback converter at different load conditions. The measured efficiency is 89% when the output power is 1 [kW].

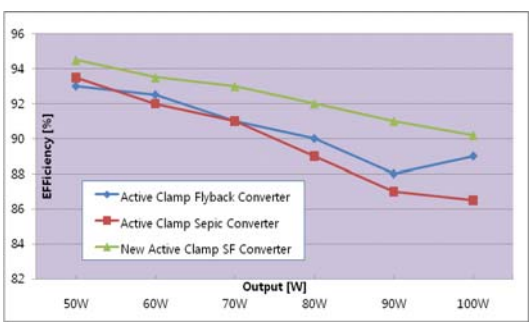

Fig. 15 The efficiency comparison of the proposed active clamp sepic-flyback converter and the conventional converters

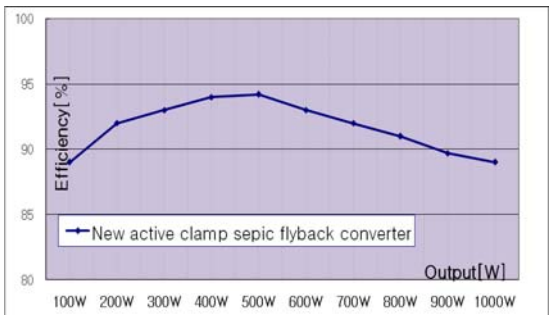

Fig. 16 The efficiency of the proposed 1 [kW] active clamp sepic-flyback converter

4. Conclusions

In this paper, we proposed a new active clamp sepic-flyback DC-DC converter for PEM fuel cell applications. The converter is a superposition of a sepic converter mode and a flyback converter mode.

The incorporation of the active clamp circuit into the sepic-flyback converter topology provides a mechanism for achieving ZVS for both the main and auxiliary switches.

Based on experimental results, the main switch and diode in this circuit were operated with soft-switching characteristics. The efficiency of the proposed sepic-flyback converter is about 89% at the rated output power. In addition, the maximum efficiency of the proposed converter was measured at about 94% at 500 [W] load. Therefore, test results show that the new active clamp sepic-flyback converter increases the overall efficiency over a conventional active clamp flyback converter and active clamp sepic converter. As a result, the proposed new active clamp sepic-flyback converter is a good candidate for use as a boost converter to improve efficiency in a fuel cell generation system.

References

[1] A. M. Tuckey, J. N. Krase, "A low-cost inverter for domestic fuel cell applications", *Proceedings of IEEE 33rd Annual. Power Electronics Specialists Conf. (PESC'02)*, Vol. 1, pp. 339–346, June 23–27, 2002.

[2] Jin Wang, Fang Z. Peng, Joel Anderson, Alan Joseph, Ryan Buffenbarger, "Low Cost Fuel Cell Converter System for

Residential Power Generation", *IEEE Trans. Power Electronics*, Vol. 19, No. 5, pp. 1315-1322, Sept. 2004.

[3] R. Watson, G. C. Hua, F. C. Lee, "Characterization of an active clamp flyback topology for Power Factor Correction Applications", *Proceedings of IEEE APEC*, pp. 412-418, 1994.

[4] Robert W. Erickson, Dragan Maksimovic, "Fundamental of Power Electronics", *International Thomson publishing*, 2001.

[5] I. D. Jitaru, S. B. Galateanu, "Small Signal Characterization of the Forward-Flyback Converters with Active Clamp", *IEEE-APEC Conf. Rec*., Vol. 2, pp.626-632, 1998.

[6] Dhaval Dalal, "Design Consideration for Active Clamp and Reset Technique", Application handbook, Unitrode.

[7] G.Spiazzi, L. Rosseito, P. Mattavelli, "Design optimization of soft switched insulated DC/DC converter with active voltage clamp", *Proceedings of IEEE IAS Annual Meeting*, pp. 2348-2355, 1996.

[8] Bor-Ren Lin, Fang-Yu Hsieh, "Soft-switching zeta-flyback converter with a buck-boost type active clamp", *IEEE Trans. Industrial Electronics*, Vol. 54, No. 5, pp 2813-2822, Oct. 2007.

[9] Changrong Liu, Jih-Sheng Lai, "Low frequency current ripple reduction technique with active control in a fuel cell power system with inverter load", *IEEE Trans. Power Electronics*, Vol. 22, No. 4, pp. 1429-1436, July 2007.

[10] Rajesh Gopinath, Jae-Hong Hahn, Prasad N. Enjeti, Mark B. Yeary, Jo W. Howze, "Development of a low cost fuel cell inverter system with control", *IEEE Trans. Power Electronics*, Vol. 19, No. 5, pp. 1256-1262, Sept. 2004.

Won-Cheol Lee was born in 1977. He received his B.S. and M.S. degrees in Electrical Engineering from Sungkyunkwan University, Korea, in 2003 and 2005, respectively. Since 2005, he has been working towards his Ph.D. degree. His main research interests are PWM converters, inverters, and motor drives.

Su-Jin Jang was born in Korea, in 1976. He received his M.S. and Ph.D. degrees Energy System Engineering from Sungkyunkwan University, Suwon, Korea, in 2004 and 2008, respectively. Currently, he is working in Hyosung. His research interests include fuel cell generation systems and regeneration inverter systems.

Soo-Seok Kim was born in Korea in 1959. He received his B.S. degree in Electrical Engineering from Seoul National University of Technology, Korea, in 1984, and his M.S. and Ph.D. degrees in Electrical Engineering from Hanyang University, Seoul, Korea, in 1989 and 1999, respectively. From 1984, he has been working in the Department of Electrical Engineering, Seoul National University of Technology. His research interests include dc−dc converters for fuel cells.

Su-Won Lee received his B.S., M.S., and Ph.D. degrees in all electrical engineering from Chonbuk National University, Korea in 1991, 1993, and 1998 respectively. He was a Research Professor with BK21 Kunsan National University from 2001 to 2006. He was a Research Professor with Institute of TMS Information Technology at Yonsei University from 2006 to 2008. Currently, he is a research professor with Center for Advanced IT HRD with Close Industry Cooperation at Sungkyunkwan University. His research interests include bi-directional dc/dc converter, inverter control and renewable energy based distributed generation system.

Chung-Yuen Won was born in Korea in 1955. He received his B.S degree in Electrical Engineering from Sungkyunkwan University, Suwon, Korea, in 1978, and the M.S. and Ph.D. degrees in Electrical Engineering from Seoul National University, Seoul, Korea, in 1980 and 1988, respectively. From 1990 to 1991, he was with the Department of Electrical Engineering, University of Tennessee, Knoxville, as a Visiting Professor. Since 1988, he has been with the faculty of Sungkyunkwan University, where he is currently a Professor in the School of Information and Communication Engineering; also he is a dean in the department of photovoltaic system engineering. His research interests include dc-dc converters for fuel cells, electro-magnetics modeling and prediction for motor drives, and control systems for rail power delivery applications.